Applied Mathematical Modelling 77 (2020) 585–601

Contents lists available at ScienceDirect

Applied Mathematical Modelling

journal homepage: www.elsevier.com/locate/apm

Stress intensity factor for bonded dissimilar materials weakened by multiple cracks

K.B. Hamzah[a,d], N.M.A. Nik Long[a,b,*], N. Senu[a,b], Z.K. Eshkuvatov[c]

[a] Laboratory of Computational Sciences and Mathematical Physics, Institute for Mathematical Research, Universiti Putra Malaysia, Serdang, Selangor 43400, Malaysia
[b] Mathematics Department, Faculty of Science, Universiti Putra Malaysia, Serdang, Selangor 43400, Malaysia
[c] Faculty of Science and Technology, Universiti Sains Islam Malaysia, NegeriSembilan 71800, Malaysia
[d] Fakulti Teknologi Kejuruteraan Mekanikal dan Pembuatan, Universiti Teknikal Malaysia Melaka, Hang Tuah Jaya, Durian Tunggal, Melaka 76100, Malaysia

ARTICLE INFO

Article history:
Received 4 April 2019
Revised 8 July 2019
Accepted 25 July 2019
Available online 7 August 2019

Keywords:
Stress intensity factors
Bonded dissimilar materials
Complex variable function
Hypersingular integral equation

ABSTRACT

The new hypersingular integral equations (HSIEs) for the multiple cracks problems in both upper and lower parts of the bonded dissimilar materials are formulated using the modified complex potential method, and with the help of the continuity conditions of the resultant force function and displacement. The crack opening displacement is the unknown and the traction along the crack as the right term of the equations. The appropriate quadrature formulas are used in solving the obtained HSIEs for the unknown coefficients. Numerical results for the multiple inclined or circular arc cracks subjected to the remote shear stress are presented.

1. Introduction

The stability and safety of the materials are very important in engineering structures, and the existence of crack may jeopardise the materials strength. The inclined and arc-like cracks problems appear in many types of materials or engineering structures. The stress intensity factors (SIF) at the crack tips can be used to determine the stability behavior of bodies or materials containing cracks or flaws. Many researchers have dealt and analysed the inclined or arc-like cracks problems in an infinite plane [1–4], a half plane [5–9] or a bonded dissimilar materials [10–12]. For the cracks problems in an infinite plane and a half plane elasticity, the HSIEs [1,13], singular integral equations [14,15] and Fredholm integral equations [16,17] were proposed.

The interaction between two cracks in circular position in an infinite plane effected the value of nondimensional SIF at the cracks tips [4]. The nondimensional SIF for the single and multiple circular arc cracks in a half plane are influenced by the position of the cracks, the distance between the cracks, and the distance between the cracks and the boundary [8]. The Mode I and Mode II nondimensional SIF for the parallel cracks in bonded dissimilar materials mainly depend on the crack configurations, elastic constant ratio and types of stresses [18]. The nondimensional SIF at the crack tip for a single crack in the upper part of bonded dissimilar materials depends on the various remote stresses, the elastic constants ratio, the crack geometries and the distance between the crack and the boundary [19].

* Corresponding author at: Laboratory of Computational Sciences and Mathematical Physics, Institute for Mathematical Research, Universiti Putra Malaysia, Serdang, Selangor 43400, Malaysia.
E-mail addresses: khairum@utem.edu.my (K.B. Hamzah), nmasri@upm.edu.my (N.M.A. Nik Long), norazak@upm.edu.my (N. Senu), zainidin@usim.edu.my (Z.K. Eshkuvatov).

https://doi.org/10.1016/j.apm.2019.07.063
0307-904X/

The crack problems in bonded dissimilar materials were discussed in recent decades. Chen [10] presented the Fredholm integral equations method for finding the nondimensional stress intensity factors (SIF) for multiple crack problems in bonded dissimilar materials. Chen and Hasebe [11] used a logarithmic singular kernel to calculate the nondimensional SIF for a circular arc crack lies in the upper half of bonded dissimilar materials. Isida and Noguchi [12] analysed the crack problems in bonded dissimilar materials by using the body force method. They excluded the interface cracks and singularity problems for cracks terminating at the interface. Yu et al. [20] used the interaction integral methods to investigate the mixed-mode SIF for crack problems in bonded dissimilar materials. Hamzah et al. [21] investigated the nondimensional SIF for the multiple cracks in the upper part of bonded dissimilar materials by using hypersingular integral equation. Li and Viola [22] used the complex potential technique to investigate the effect of interface crack lies along the central between two bonded dissimilar materials. Ghajar et al. [23] presented the effect of Poisson's ratio on mixed-mode SIF of the interface crack in bonded dissimilar materials by using the displacement fields method. Serier et al. [24] identified the effect of interaction between an interfacial main crack and a subinterfacial microcrack in bonded dissimilar materials by using finite element method. Wang and Waisman [25] presented an extended finite element method to analyze the materials dependency for the interface cracks in bonded dissimilar materials. Itou [26] combined the solution for an inner and an outer collinear cracks to calculate the nondimensional SIF for the collinear interface cracks in bonded dissimilar materials. Paggi and Reinoso [27] investigated the competition between crack penetration and deflection at the interface of bonded dissimilar materials by using finite element method based on the monolithic fully implicit solution strategy. Lan et al. [28] used the proportional crack opening displacements to compute the nondimensional SIF for two-dimensional interface cracks, three-dimensional penny-shaped cracks and circumferential surface cracks in bonded dissimilar materials. Cordeiro and Leonel [29] developed the mechanical modelling for three dimensional cracked structural components by using the isogeometric dual boundary element method. e Andrade and Leonel [30] used the dual boundary element method to calculate the nondimensional SIF for two dimensional multiple cracks propagation in bonded dissimilar materials. Complex variable function method was used to solve the crack problems [31], to investigate the nondimensional SIF behavior [32] and to analyse the interaction of the cracks [33] in bonded dissimilar materials.

In this paper the multiple cracks problems in both upper and lower parts of bonded dissimilar materials subjected to the remote shear stress $\sigma_{x_1} = \sigma_{x_2} = p$ are considered. The problem concerns the proposition of analytical approach for solving engineering structure problems with dissimilar materials, which are perfectly bonded and subjected to an initial crack distribution. The problem is formulated into the new HSIEs, which later to be solved and enable us to investigate the behavior of nondimensional SIF at the cracks tips.

2. Mathematical formulation

The complex variable function method introduced by Muskhelishvili [34] are used in solving the cracks problems. The stress components (σ_x, σ_y, σ_{xy}), the resultant force function (X, Y), and the displacements (u, v) are expressed in terms of two complex potential functions $\phi(z)$ and $\psi(z)$ as follows

$$\sigma_y - \sigma_x + 2i\sigma_{xy} = 2[\bar{z}\phi''(z) + \psi'(z)] \tag{1}$$

$$f = -Y + iX = \phi(z) + z\overline{\phi'(z)} + \overline{\psi(z)} \tag{2}$$

$$2G(u + iv) = \kappa\phi(z) - z\overline{\phi'(z)} - \overline{\psi(z)} \tag{3}$$

where G is shear modulus of elasticity, $\kappa = 3 - 4\nu$ for plane strain, $\kappa = (3 - \nu)/(1 + \nu)$ for plane stress and ν is Poisson's ratio. A derivative in a specified direction of Eq. (2) with respect to z, which yields the normal (N) and tangential (T) components of traction along the segment $\overline{z, z + dz}$, is defined as follows

$$\frac{d}{dz}\{-Y + iX\} = \phi'(z) + \overline{\phi'(z)} + \frac{d\bar{z}}{dz}\left[z\overline{\phi''(z)} + \overline{\psi'(z)}\right] = N + iT. \tag{4}$$

Consider two cracks lie in the upper and lower half of the bonded dissimilar materials (Fig. 1). The condition for remote stress in bonded dissimilar materials is

$$\varepsilon_{x_1} = \varepsilon_{x_2}, \tag{5}$$

where ε_{x_1} and ε_{x_2} are the stress component for the upper and lower half of bonded dissimilar materials, respectively. Those stress can be expressed as

$$\varepsilon_{x_1} = \frac{1}{E_1}\left(\sigma^{\infty}_{x_1} - \nu_1\sigma^{\infty}_{y_1}\right), \quad \varepsilon_{x_2} = \frac{1}{E_2}\left(\sigma^{\infty}_{x_2} - \nu_2\sigma^{\infty}_{y_2}\right) \tag{6}$$

where $E_1 = 2G_1(1 + \nu_1)$ and $E_2 = 2G_2(1 + \nu_2)$ are Young's modulus of elasticity and ν_1 and ν_2 are Poisson's ratio for upper and lower half of bonded dissimilar materials, respectively. If the remote stress $\sigma^{\infty}_{y_1} = \sigma^{\infty}_{y_2} = 0$, then the stress component is reduced to

$$\frac{1}{E_1}\sigma^{\infty}_{x_1} = \frac{1}{E_2}\sigma^{\infty}_{x_2}. \tag{7}$$

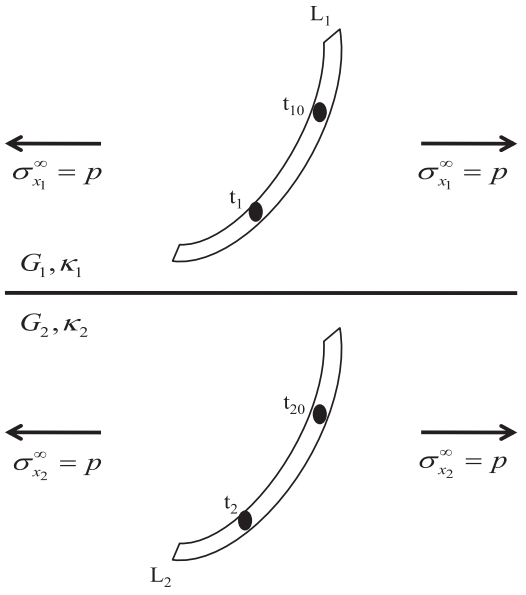

Fig. 1. Two cracks L_1 and L_2 in bonded dissimilar materials.

The modified complex potentials (MCP) for the cracks lie in the upper half of the material is defined as

$$\phi_1(z) = \phi_{1p}(z) + \phi_{1c}(z), \quad \psi_1(z) = \psi_{1p}(z) + \psi_{1c}(z), \tag{8}$$

where $\phi_{1p}(z)$ and $\psi_{1p}(z)$ are the principal parts and $\phi_{1c}(z)$ and $\psi_{1c}(z)$ are the complementary parts of the complex potentials. Whereas, for the cracks lie in the lower plane, the complex potentials are represented by $\phi_2(z)$ and $\psi_2(z)$. The principal parts of complex potentials are referred to the complex potentials for the cracks in an infinite plane. According to Nik Long and Eshkuvatov [2], complex potentials for the crack L in an infinite plane modeled by the distribution of crack opening displacement (COD) function $g(t)$ can be expressed by

$$\phi_{1p}(z) = \frac{1}{2\pi}\int_L \frac{g(t)dt}{t-z} \tag{9}$$

$$\psi_{1p}(z) = \frac{1}{2\pi}\int_L \frac{\overline{g(t)}dt}{t-z} + \frac{1}{2\pi}\int_L \frac{g(t)d\bar{t}}{t-z} - \frac{1}{2\pi}\int_L \frac{g(t)\bar{t}dt}{(t-z)^2} \tag{10}$$

where $g(t)$ is defined by

$$g(t) = \frac{2G}{i(\kappa+1)}\left[(u(t)+iv(t))^+ - (u(t)+iv(t))^-\right], t \in L \tag{11}$$

$(u(t)+iv(t))^+$ and $(u(t)+iv(t))^-$ denote the displacements at point t of the upper and lower crack faces, respectively.

The continuity conditions for resultant force (2) and displacement (3) are defined, respectively, as

$$\left[\phi_1(t) + t\overline{\phi_1'(t)} + \overline{\psi_1(t)}\right]^+ = \left[\phi_2(t) + t\overline{\phi_2'(t)} + \overline{\psi_2(t)}\right]^-, t \in L \tag{12}$$

$$G_2\left[\kappa_1\phi_1(t) - t\overline{\phi_1'(t)} - \overline{\psi_1(t)}\right]^+ = G_1\left[\kappa_2\phi_2(t) - t\overline{\phi_2'(t)} - \overline{\psi_2(t)}\right]^-, t \in L. \tag{13}$$

Applying Eq. (8) into Eqs. (12) and (13), the following expressions are obtainable:

$$\phi_{1c}(z) = \Gamma_1\left[z\overline{\phi_{1p}'}(z) + \overline{\psi_{1p}}(z)\right], z \in S_{\text{upper}} + L_b \tag{14}$$

$$\psi_{1c}(z) = \Gamma_2\overline{\phi_{1p}}(z) - \Gamma_1\left[z\overline{\phi_{1p}'}(z) + z^2\overline{\phi_{1p}''}(z) + z\overline{\psi_{1p}'}(z)\right], z \in S_{\text{upper}} + L_b \tag{15}$$

$$\phi_2(z) = \left(1+\Gamma_2\right)\phi_{1p}(z), z \in S_{\text{lower}} + L_b \tag{16}$$

$$\psi_2(z) = \left(\Gamma_1 - \Gamma_2\right)z\phi_{1p}'(z) + \left(1+\Gamma_1\right)\psi_{1p}, z \in S_{\text{lower}} + L_b \tag{17}$$

where $\overline{\phi_{1p}}(z) = \overline{\phi_{1p}(\bar{z})}$, L_b is boundary of two bonded half plane, S_{upper} and S_{lower} are upper and lower half plane of bonded dissimilar materials, respectively, and Γ_1, Γ_2 are bi-elastic constants defined as

$$\Gamma_1 = \frac{G_2 - G_1}{G_1 + \kappa_1 G_2}, \quad \Gamma_2 = \frac{\kappa_1 G_2 - \kappa_2 G_1}{G_2 + \kappa_2 G_1}. \tag{18}$$

In order to formulate the HSIEs for the cracks lie in both the upper and lower half of bonded dissimilar materials, we need to defined four traction components $\{N(t_0)+iT(t_0)\}_{jk}$ $(j=1,2,k=1,2)$ which consist of two groups of $N+iT$ influences. The first two tractions $\{N(t_{10})+iT(t_{10})\}_{11}$ and $\{N(t_{20})+iT(t_{20})\}_{21}$ are obtained when the observation point is placed at the point $t_{10}(t_{10}\in L_1)$ and $t_{20}(t_{20}\in L_2)$, respectively, caused by $g_1(t_1)$ at $(t_1\in L_1)$. For $\{N(t_{10})+iT(t_{10})\}_{11}$, we need to combine the principal $\{N(t_{10})+iT(t_{10})\}_{1p}$ and complementary parts $\{N(t_{10})+iT(t_{10})\}_{1c}$ of the tractions. Substituting Eqs. (9) and (10) into (4) for $\{N(t_{10})+iT(t_{10})\}_{1p}$ and substituting Eqs. (14) and (15) into (4), applying (9) and (10) for $\{N(t_{10})+iT(t_{10})\}_{1c}$. Then letting point z approaches t_{10} on the crack and changing $d\bar{z}/dz$ into $d\bar{t}_{10}/dt_{10}$, yields

$$\begin{aligned}\{N(t_{10})+iT(t_{10})\}_{11} &= \{N(t_{10})+iT(t_{10})\}_{1p}+\{N(t_{10})+iT(t_{10})\}_{1c}\\ &= \frac{1}{\pi}\neq\!\!\!\!\!\!\int_{L_1}\frac{g_1(t_1)dt_1}{(t_1-t_{10})^2}+\frac{1}{2\pi}\int_{L_1}A_1(t_1,t_{10})g_1(t_1)dt_1+\frac{1}{2\pi}\int_{L_1}A_2(t_1,t_{10})\overline{g_1(t_1)}dt_1\end{aligned}\tag{19}$$

where

$$\begin{aligned}A_1(t_1,t_{10}) &= -\frac{1}{(t_1-t_{10})^2}+\frac{1}{(\bar{t}_1-\bar{t}_{10})^2}\frac{d\bar{t}_1}{dt_1}\frac{d\bar{t}_{10}}{dt_{10}}\\ &\quad+\Gamma_1\Bigg[\frac{1}{(t_1-\bar{t}_{10})^2}+\frac{2(\bar{t}_{10}-\bar{t}_1)}{(t_1-\bar{t}_{10})^3}+\frac{d\bar{t}_{10}}{dt_{10}}\Bigg(\frac{2(2t_{10}-3\bar{t}_{10}+\bar{t}_1)}{(t_1-\bar{t}_{10})^3}-\frac{6(\bar{t}_{10}-\bar{t}_1)(\bar{t}_{10}-t_{10})}{(t_1-\bar{t}_{10})^4}-\frac{1}{(t_1-\bar{t}_{10})^2}\Bigg)\\ &\quad+\frac{d\bar{t}_1}{dt_1}\Bigg(\frac{1}{(\bar{t}_1-t_{10})^2}+\frac{1}{(t_1-\bar{t}_{10})^2}\Bigg)-\frac{d\bar{t}_1}{dt_1}\frac{d\bar{t}_{10}}{dt_{10}}\Bigg(\frac{1}{(t_1-\bar{t}_{10})^2}+\frac{2(\bar{t}_{10}-t_{10})}{(t_1-\bar{t}_{10})^3}\Bigg)\Bigg]+\Gamma_2\frac{d\bar{t}_{10}}{dt_{10}}\frac{1}{(t_1-\bar{t}_{10})^2}\\ A_2(t_1,t_{10}) &= \frac{1}{(\bar{t}_1-\bar{t}_{10})^3}\Bigg(\frac{d\bar{t}_1}{dt_1}+\frac{d\bar{t}_{10}}{dt_{10}}\Bigg)-\frac{2(t_1-t_{10})}{(\bar{t}_1-\bar{t}_{10})^3}\frac{d\bar{t}_1}{dt_1}\frac{d\bar{t}_{10}}{dt_{10}}\\ &\quad+\Gamma_1\Bigg[\frac{1}{(\bar{t}_1-t_{10})^2}+\frac{1}{(t_1-\bar{t}_{10})^2}-\frac{d\bar{t}_{10}}{dt_{10}}\Bigg(\frac{1}{(t_1-\bar{t}_{10})^2}+\frac{2(\bar{t}_{10}-t_{10})}{(t_1-\bar{t}_{10})^3}\Bigg)+\frac{d\bar{t}_1}{dt_1}\Bigg(\frac{1}{(\bar{t}_1-t_{10})^2}+\frac{2(t_{10}-t_1)}{(\bar{t}_1-t_{10})^3}\Bigg)\Bigg].\end{aligned}$$

For $\{N(t_{20})+iT(t_{20})\}_{21}$, substituting Eqs. (16) and (17) into (4) and applying (9) and (10), yields

$$\{N(t_{20})+iT(t_{20})\}_{21}=(1+\Gamma_2)\frac{1}{\pi}\int_{L_2}\frac{g_1(t_1)dt_1}{(t_1-t_{20})^2}+\frac{1}{2\pi}\int_{L_2}B_1(t_1,t_{20})g_1(t_1)dt_1+\frac{1}{2\pi}\int_{L_2}B_2(t_1,t_{20})\overline{g_1(t_1)}dt_1\tag{20}$$

where

$$\begin{aligned}B_1(t_1,t_{20}) &= -(1+\Gamma_2)\frac{1}{(t_1-t_{20})^2}+(1+\Gamma_1)\Bigg(\frac{1}{(\bar{t}_1-\bar{t}_{20})^2}\Bigg)\frac{d\bar{t}_1}{dt_1}\frac{d\bar{t}_{20}}{dt_{20}}\\ B_2(t_1,t_{20}) &= \frac{1}{(\bar{t}_1-\bar{t}_{20})^2}\Bigg((1+\Gamma_2)\frac{d\bar{t}_1}{dt_1}+(1+\Gamma_1)\frac{d\bar{t}_{20}}{dt_{20}}\Bigg)\\ &\quad+(1+\Gamma_2)\Bigg(\frac{2t_{20}}{(\bar{t}_1-\bar{t}_{20})^3}\Bigg)\frac{d\bar{t}_1}{dt_1}\frac{d\bar{t}_{20}}{dt_{20}}-(1+\Gamma_1)\Bigg(\frac{2t_1}{(\bar{t}_1-\bar{t}_{20})^3}\Bigg)\frac{d\bar{t}_1}{dt_1}\frac{d\bar{t}_{20}}{dt_{20}}\\ &\quad+(\Gamma_1-\Gamma_2)\Bigg(\frac{1}{(\bar{t}_1-\bar{t}_{20})^2}+\frac{2\bar{t}_{20}}{(\bar{t}_1-\bar{t}_{20})^3}\Bigg)\frac{d\bar{t}_1}{dt_1}\frac{d\bar{t}_{20}}{dt_{20}}.\end{aligned}$$

Whereas, the second two tractions $\{N(t_{10})+iT(t_{10})\}_{12}$ and $\{N(t_{20})+iT(t_{20})\}_{22}$ are obtained when the observation point is placed at the point $t_{10}(t_{10}\in L_1)$ and $t_{20}(t_{20}\in L_2)$, respectively, caused by $g_2(t_2)$ at $(t_2\in L_2)$. In this process we need to introduce two bi-elastic constants define as

$$\Pi_1=\frac{G_1-G_2}{G_2+\kappa_2G_1},\quad \Pi_2=\frac{\kappa_2G_1-\kappa_1G_2}{G_1+\kappa_1G_2}\tag{21}$$

which is evaluated by changing the subscript 1 to 2 and 2 to 1 in Γ_1 and Γ_2. Similarly, for $\{N(t_{10})+iT(t_{10})\}_{12}$, we need to combine the principal and complementary parts of the tractions. Substituting Eqs. (9), (10), (14) and (15) into (4) yields

$$\{N(t_{10})+iT(t_{10})\}_{12}=\frac{1}{\pi}\int_{L_2}\frac{g_2(t_2)dt_2}{(t_2-t_{10})^2}+\frac{1}{2\pi}\int_{L_2}D_1(t_2,t_{10})g_2(t_2)dt_2+\frac{1}{2\pi}\int_{L_2}D_2(t_2,t_{10})\overline{g_2(t_2)}dt_2\tag{22}$$

where

$$D_1(t_2,t_{10}) = -\frac{1}{(t_2-t_{10})^2}+\frac{1}{(\bar{t}_2-\bar{t}_{10})^2}\frac{d\bar{t}_2}{dt_2}\frac{d\bar{t}_{10}}{dt_{10}} + \Pi_1\Big[\frac{1}{(t_2-\bar{t}_{10})^2}+\frac{2(\bar{t}_{10}-\bar{t}_2)}{(t_2-\bar{t}_{10})^3}+\frac{d\bar{t}_{10}}{dt_{10}}\Big(\frac{2(2t_{10}-3\bar{t}_{10}+\bar{t}_2)}{(t_2-\bar{t}_{10})^3}-\frac{6(\bar{t}_{10}-\bar{t}_2)(\bar{t}_{10}-t_{10})}{(t_2-\bar{t}_{10})^4}-\frac{1}{(t_2-\bar{t}_{10})^2}\Big) + \frac{d\bar{t}_2}{dt_2}\Big(\frac{1}{(\bar{t}_2-t_{10})^2}+\frac{1}{(t_2-\bar{t}_{10})^2}\Big)+\frac{d\bar{t}_2}{dt_2}\frac{d\bar{t}_{10}}{dt_{10}}\Big(-\frac{1}{(t_2-\bar{t}_{10})^2}-\frac{2(\bar{t}_{10}-t_{10})}{(t_2-\bar{t}_{10})^3}\Big)\Big]+\Pi_2\frac{d\bar{t}_{10}}{dt_{10}}\frac{1}{(t_2-\bar{t}_{10})^2}$$

$$D_2(t_2,t_{10}) = \frac{1}{(\bar{t}_2-\bar{t}_{10})^3}\Big(\frac{d\bar{t}_2}{dt_2}+\frac{d\bar{t}_{10}}{dt_{10}}\Big)-\frac{2(t_2-t_{10})}{(\bar{t}_2-\bar{t}_{10})^3}\frac{d\bar{t}_2}{dt_2}\frac{d\bar{t}_{10}}{dt_{10}} + \Pi_1\Big[\frac{1}{(\bar{t}_2-t_{10})^2}+\frac{1}{(t_2-\bar{t}_{10})^2}+\frac{d\bar{t}_{10}}{dt_{10}}\Big(-\frac{1}{(t_2-\bar{t}_{10})^2}-\frac{2(\bar{t}_{10}-t_{10})}{(t_2-\bar{t}_{10})^3}\Big) + \frac{d\bar{t}_2}{dt_2}\Big(\frac{1}{(\bar{t}_2-t_{10})^2}+\frac{2(t_{10}-t_2)}{(\bar{t}_2-t_{10})^3}\Big)\Big].$$

For $\{N(t_{20})+iT(t_{20})\}_{22}$, substituting Eqs. (16) and (17) into (4) and applying (9) and (10), yields

$$\{N(t_{20})+iT(t_{20})\}_{22} = (1+\Pi_2)\frac{1}{\pi}\Xint=_{L_2}\frac{g_2(t_2)dt_2}{(t_2-t_{20})^2}+\frac{1}{2\pi}\int_{L_2}E_1(t_2,t_{20})g_2(t_2)dt_2+\frac{1}{2\pi}\int_{L_2}E_2(t_2,t_{20})\overline{g_2(t_2)}dt_2 \tag{23}$$

where

$$E_1(t_2,t_{20}) = -(1+\Pi_2)\frac{1}{(t_2-t_{20})^2}+(1+\Pi_1)\Big(\frac{1}{(\bar{t}_2-\bar{t}_{20})^2}\Big)\frac{d\bar{t}_2}{dt_2}\frac{d\bar{t}_{20}}{dt_{20}}$$

$$E_2(t_2,t_{20}) = \frac{1}{(\bar{t}_2-\bar{t}_{20})^2}\Big((1+\Pi_2)\frac{d\bar{t}_2}{dt_2}+(1+\Pi_1)\frac{d\bar{t}_{20}}{dt_{20}}\Big) + \Big[(1+\Pi_2)\Big(\frac{2t_{20}}{(\bar{t}_2-\bar{t}_{20})^3}\Big)-(1+\Pi_1)\Big(\frac{2t_2}{(\bar{t}_2-\bar{t}_{20})^3}\Big)+(\Pi_1-\Pi_2)\Big(\frac{1}{(\bar{t}_2-\bar{t}_{20})^2}+\frac{2\bar{t}_{20}}{(\bar{t}_2-\bar{t}_{20})^3}\Big)\Big]\frac{d\bar{t}_2}{dt_2}\frac{d\bar{t}_{20}}{dt_{20}}.$$

The HSIEs for the system of two cracks L_1 and L_2 lie in the upper and lower half of bonded dissimilar materials is obtained by using two groups of $N+iT$ influences as follows

$$\begin{aligned}\{\widetilde{N}(t_{10})+i\widetilde{T}(t_{10})\}_1 &= \{N(t_{10})+iT(t_{10})\}_{11}+\{N(t_{10})+iT(t_{10})\}_{12}\\ &= \frac{1}{\pi}\Xint=_{L_1}\frac{g_1(t_1)dt_1}{(t_1-t_{10})^2}+\frac{1}{2\pi}\int_{L_1}A_1(t_1,t_{10})g_1(t_1)dt_1\\ &\quad+\frac{1}{2\pi}\int_{L_1}A_2(t_1,t_{10})\overline{g_1(t_1)}dt_1+\frac{1}{\pi}\int_{L_2}\frac{g_2(t_2)dt_2}{(t_2-t_{10})^2}\\ &\quad+\frac{1}{2\pi}\int_{L_2}D_1(t_2,t_{10})g_2(t_2)dt_2+\frac{1}{2\pi}\int_{L_2}D_2(t_2,t_{10})\overline{g_2(t_2)}dt_2\end{aligned} \tag{24}$$

and

$$\begin{aligned}\{\widetilde{N}(t_{20})+i\widetilde{T}(t_{20})\}_2 &= \{N(t_{20})+iT(t_{20})\}_{22}+\{N(t_{20})+iT(t_{20})\}_{21}\\ &= (1+\Pi_2)\frac{1}{\pi}\Xint=_{L_2}\frac{g_2(t_2)dt_2}{(t_2-t_{20})^2}+\frac{1}{2\pi}\int_{L_2}E_1(t_2,t_{20})g_2(t_2)dt_2\\ &\quad+\frac{1}{2\pi}\int_{L_2}E_2(t_2,t_{20})\overline{g_2(t_2)}dt_2+(1+\Gamma_2)\frac{1}{\pi}\int_{L_2}\frac{g_1(t_1)dt_1}{(t_1-t_{20})^2}\\ &\quad+\frac{1}{2\pi}\int_{L_2}B_1(t_1,t_{20})g_1(t_1)dt_1+\frac{1}{2\pi}\int_{L_2}B_2(t_1,t_{20})\overline{g_1(t_1)}dt_1.\end{aligned} \tag{25}$$

Note that if $G_1=G_2$ HSIEs (24) and (25) reduce to the HSIEs for the cracks in an infinite plane [1].
In order to solve the HSIEs (24) and (25), the function $g_j(t_j)$ is mapped on a real axis s with an interval $2a$ as follows

$$g_j(t_j)|_{t_j=t_j(s_j)} = \sqrt{a_j^2-s_j^2}H_j(s_j),\ j=1,2 \tag{26}$$

where $H_j(s_j) = H_{j1}(s_j) + iH_{j2}(s_j)$, with the following quadrature formulas

$$\frac{1}{\pi}\int_{-a}^{a} \frac{\sqrt{a^2 - s^2}H(s)ds}{(s - s_0)^2} \simeq \sum_{j=1}^{M+1} W_j(s_0)H(s_j), \quad (|s_0| < a) \tag{27}$$

$$\frac{1}{\pi}\int_{-a}^{a} \sqrt{a^2 - s^2}H(s)ds \simeq \frac{1}{M+2}\sum_{j=1}^{M+1}(a^2 - s_j^2)H(s_j), \tag{28}$$

where $M \in \mathbb{Z}^+$,

$$s_j = a\cos\left(\frac{j\pi}{M+2}\right), \quad j = 1, 2, \ldots, M+1$$

and

$$W_j(s_0) = -\frac{2}{M+2}\sum_{n=0}^{M}(n+1)\sin\left(\frac{j\pi}{M+2}\right)\sin\left(\frac{(n+1)j\pi}{M+2}\right)U_n\left(\frac{s_{j0}}{a}\right)$$

and the observation points

$$s_0 = s_{j0,k} = a\cos\left(\frac{k\pi}{M+2}\right), \quad k = 1, 2, \ldots, M+1.$$

Here $U_n(t)$ is a Chebyshev polynomial of the second kind, defined by

$$U_n(t) = \frac{\sin((n+1)\theta)}{\sin\theta}, \text{where } t = \cos\theta. \tag{29}$$

3. Numerical results and discussions

Stress intensity factor (SIF) at the crack tips A_j and B_j are defined as

$$\begin{aligned}(K_1 - iK_2)_{A_j} &= \sqrt{2\pi}\lim_{t\to t_{A_j}}\sqrt{|t - t_{A_j}|}g_1'(t_1), \quad j = 1, 2\\ &= \sqrt{2\pi}\lim_{s\to s_{A_j}}\sqrt{|s - s_{A_j}|}\left[\frac{-s_1H_1(s_1)}{\sqrt{a_1^2 - s_1^2}}e^{-i\theta_{A_j}}\right]\\ &= \sqrt{a_1\pi}F_{A_j}\end{aligned} \tag{30}$$

$$\begin{aligned}(K_1 - iK_2)_{B_j} &= \sqrt{2\pi}\lim_{t\to t_{B_j}}\sqrt{|t - t_{B_j}|}g_2'(t_2), \quad j = 1, 2\\ &= \sqrt{2\pi}\lim_{s\to s_{B_j}}\sqrt{|s - s_{B_j}|}\left[\frac{-s_2H_2(s_2)}{\sqrt{a_2^2 - s_2^2}}e^{-i\theta_{B_j}}\right]\\ &= \sqrt{a_2\pi}F_{B_j}\end{aligned} \tag{31}$$

where the nondimensional SIF at cracks tips F_{A_j} and F_{B_j} defined as

$$F_{A_1} = H_1(-a_1)e^{-i\theta_{A_1}}, \quad F_{A_2} = H_1(a_1)e^{-i\theta_{A_2}},$$

$$F_{B_1} = H_2(-a_2)e^{-i\theta_{B_1}}, \quad F_{B_2} = H_2(a_2)e^{-i\theta_{B_2}}.$$

3.1. Two inclined cracks

Consider two parallel inclined cracks (Fig. 2(a)) and two inclined cracks in series (Fig. 2(b)) subjected to remote shear stress $\sigma_{x_1} = \sigma_{x_2} = p$ and $\nu_1 = \nu_2 = 0.3$.

Table 1 displays the nondimensional SIF at the crack tips when $\alpha_1 = \alpha_2 = 90^o$ with different values of elastic constant ratio G_2/G_1 where R and h are defined as in Fig. 2(a). Our results are in good agreement with those of Chen [10] for Mode I nondimensional SIF, F_1, whereas Mode II nondimensional SIF, F_2, equal to zero at all crack tips. Fig. 3 shows the nondimensional SIF at all crack tips when $R/h = 0.9$ and $\alpha_1 = \alpha_2$ varies (Fig. 2(a)). It is found that as $\alpha_1 = \alpha_2$ increases F_1 increases at

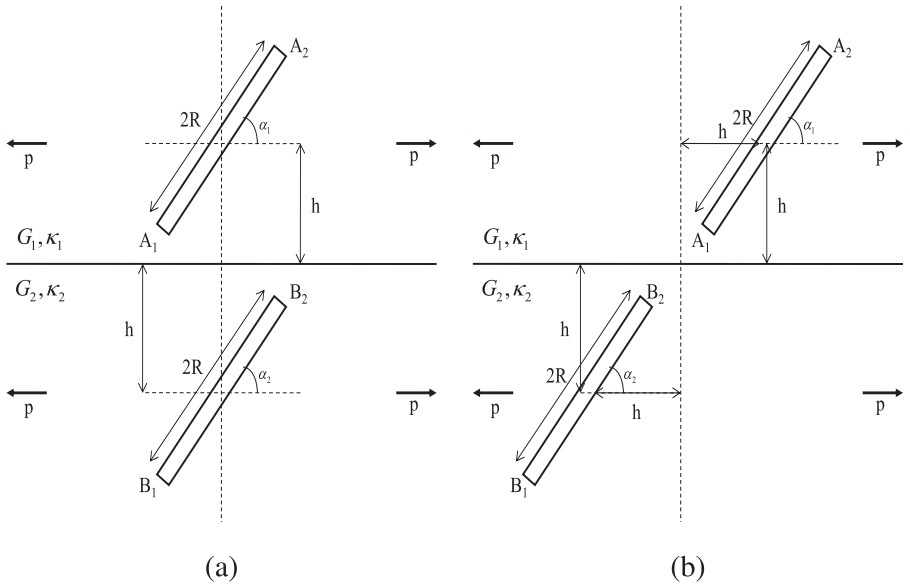

Fig. 2. Two inclined cracks in bonded dissimilar materials subjected to shear stress $\sigma_{x_1} = \sigma_{x_2} = p$.

Table 1
Nondimensional SIF for the two parallel inclined cracks when $\alpha_1 = \alpha_2 = 90^o$ (Fig. 2(a)).

G_2/G_1	SIF	R/h								
		0.1	0.2	0.3	0.4	0.5	0.6	0.7	0.8	0.9
1.0	F_{1A_1} [a]	1.0013	1.0055	1.0138	1.0272	1.0480	1.0804	1.1333	1.2289	1.4539
	F_{1A_1} [b]	1.0010	1.0060	1.0140	1.0270	1.0480	1.0800	1.1330	1.2290	1.4540
	F_{1A_2} [a]	1.0011	1.0045	1.0101	1.0178	1.0279	1.0409	1.0578	1.0810	1.1173
	F_{1A_2} [b]	1.0010	1.0050	1.0100	1.0180	1.0280	1.0410	1.0580	1.0810	1.1170
	F_{1B_1} [a]	1.0011	1.0045	1.0101	1.0178	1.0279	1.0409	1.0578	1.0810	1.1173
	F_{1B_1} [b]	1.0010	1.0050	1.0100	1.0180	1.0280	1.0410	1.0580	1.0810	1.1170
	F_{1B_2} [a]	1.0013	1.0055	1.0138	1.0272	1.0480	1.0804	1.1333	1.2289	1.4539
	F_{1B_2} [b]	1.0010	1.0060	1.0140	1.0270	1.0480	1.0800	1.1330	1.2290	1.4540
2.0	F_{1A_1} [a]	1.0010	1.0046	1.0115	1.0233	1.0421	1.0728	1.1254	1.2256	1.4768
	F_{1A_1} [b]	1.0010	1.0050	1.0110	1.0220	1.0390	1.0660	1.1110	1.1960	1.4040
	F_{1A_2} [a]	1.0009	1.0036	1.0083	1.0147	1.0234	1.0350	1.0509	1.0740	1.1128
	F_{1A_2} [b]	1.0010	1.0040	1.0090	1.0150	1.0250	1.0370	1.0540	1.0780	1.1180
	F_{1B_1} [a]	1.0015	1.0061	1.0135	1.0236	1.0367	1.0534	1.0752	1.1051	1.1528
	F_{1B_1} [b]	1.0010	1.0060	1.0120	1.0220	1.0330	1.0480	1.0670	1.0920	1.1290
	F_{1B_2} [a]	1.0017	1.0076	1.0190	1.0376	1.0668	1.1128	1.1885	1.3275	1.6625
	F_{1B_2} [b]	1.0020	1.0070	1.0170	1.0340	1.0590	1.0980	1.1590	1.2670	1.5120
5.0	F_{1A_1} [a]	1.0008	1.0035	1.0092	1.0191	1.0359	1.0647	1.1167	1.2216	1.5027
	F_{1A_1} [b]	1.0010	1.0040	1.0090	1.0170	1.0300	1.0520	1.0900	1.1650	1.3580
	F_{1A_2} [a]	1.0007	1.0027	1.0063	1.0115	1.0187	1.0288	1.0436	1.0662	1.1074
	F_{1A_2} [b]	1.0010	1.0030	1.0080	1.0140	1.0230	1.0370	1.0560	1.0840	1.1330
	F_{1B_1} [a]	1.0020	1.0078	1.0173	1.0300	1.0464	1.0672	1.0942	1.1313	1.1916
	F_{1B_1} [b]	1.0010	1.0070	1.0160	1.0270	1.0420	1.0600	1.0820	1.1120	1.1550
	F_{1B_2} [a]	1.0023	1.0101	1.0252	1.0502	1.0896	1.1523	1.2565	1.4503	1.9296
	F_{1B_2} [b]	1.0020	1.0090	1.0210	1.0420	1.0730	1.1190	1.1920	1.3160	1.5890

[a] Current study
[b] [10]

all crack tips and F_2 decreases for $\alpha_1 = \alpha_2 < 50^o$. The increment of G_2/G_1 will decrease F_1 at crack tips A_1 and A_2 however at crack tips B_1 and B_2, F_1 increases, whereas F_2 increases at crack tips A_1 and B_1, decreases at B_2 and at A_2 does not show any significant differences.

Fig. 4 shows the nondimensional SIF for two inclined cracks in series when $R/h = 0.9$, $\alpha_2 = 45^o$ and α_1 varies (Fig. 2(b)). As α_1 increases F_1 increases at all cracks tips and F_2 decreases at crack tips B_1 and B_2, whereas at crack tips A_1 and A_2 F_2 decreases for $\alpha_1 < 50^o$. It is also observed that as G_2/G_1 increases F_1 decreases at the crack tips A_1 and A_2 and increases at B_1 and B_2, whereas F_2 decreases at crack tip A_1 and decreases at at B_1 and B_2, and does not show any significant differences at crack tip A_2.

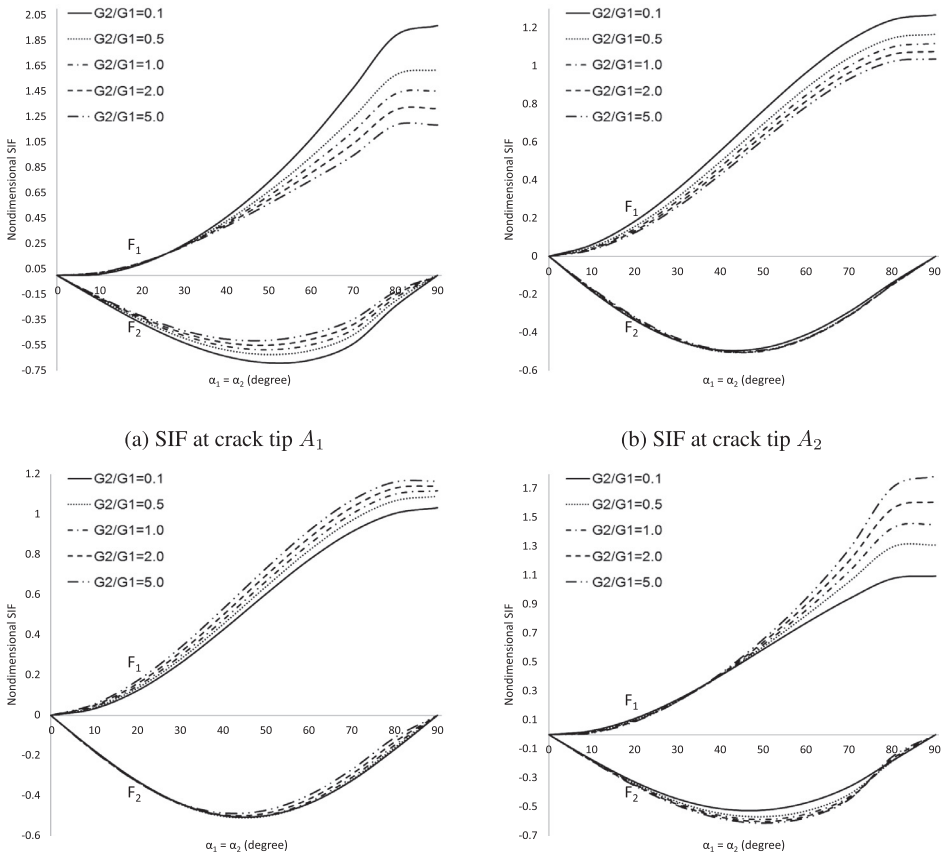

(a) SIF at crack tip A_1

(b) SIF at crack tip A_2

(c) SIF at crack tip B_1

(d) SIF at crack tip B_2

Fig. 3. Nondimensional SIF vs $\alpha_1 = \alpha_2$ with different values of G_2/G_1 for $R/h = 0.9$ (Fig. 2(a)).

3.2. Two semi circular arc cracks

Consider two semi circular arc cracks in bonded dissimilar materials as in Fig. 5. In Fig. 5(a), both cracks facing the same direction with radius R, whereas Fig. 5(b), two cracks facing the opposite direction with radius R_1 and R_2.

Fig. 6 (a) and (b) show the nondimensional SIF at crack tips A_1 and B_1 respectively when $\alpha = 90^o$ and h varies for the problem defined in Fig. 5(a). It is observed that F_1 at crack tips A_1 and B_1 are equals to F_1 at tips A_2 and B_2, respectively, whereas F_2 at crack tips A_1 and B_1 are equals to the negative of F_2 at tips A_2 and B_2, respectively. At the crack tip A_1, as h increases F_1 decreases and F_2 increases for $G_2/G_1 < 1.0$ and decreases for $G_2/G_1 \geq 1.0$, and as G_2/G_1 increases F_1 decreases and F_2 increases. Whereas at the crack tip B_1, as h increases F_1 decreases and F_2 increases, and as G_2/G_1 increases F_1 increases and F_2 decreases. For $h = 0.5R$ and α varies the nondimensional SIF at crack tips A_1 and B_1 are presented in Fig. 7. It clearly shows that F_1 increases as α increases and F_2 decreases for $\alpha > 50^o$ at all crack tips. As G_2/G_1 increases F_1 decreases and F_2 decreases for $\alpha < 70^o$ at crack tip A_1, whereas at crack tip B_1, F_1 increases and F_2 decreases.

Fig. 8 plots the nondimensional SIF versus h_1 when $R_1 = R_2$ for the problem defined in Fig. 5(b). It is found that F_1 at crack tips A_1 and B_1 are equals to F_1 at tips A_2 and B_2, respectively, whereas F_2 at crack tips A_1 and B_1 are equals to the negative of F_2 at tips A_2 and B_2, respectively. As h_1 and G_2/G_1 increase F_1 decreases and F_2 does not show any significant differences at crack tip A_1. Whereas at crack tip B_1 as h_1 and G_2/G_1 increase F_1 deceases and increases, respectively, and F_2 does not show any significant differences. Fig. 9 shows the nondimensional SIF versus R_2/R_1 when $R_1/h_2 = 0.9$ and $h_2 = 1.0$ for the problem defined in Fig. 5(b). It is observed that at crack tip A_1, as R_2/R_1 increases F_1 increases and F_2 increases for $R_2/R_1 > 0.9$, and as G_2/G_1 increases F_1 decreases and F_2 does not show any significant differences. Whereas at crack tip B_1, as R_2/R_1 increases F_1 increases and F_2 increases for $R_2/R_1 < 0.9$, and as G_2/G_1 increases F_1 and F_2 increase.

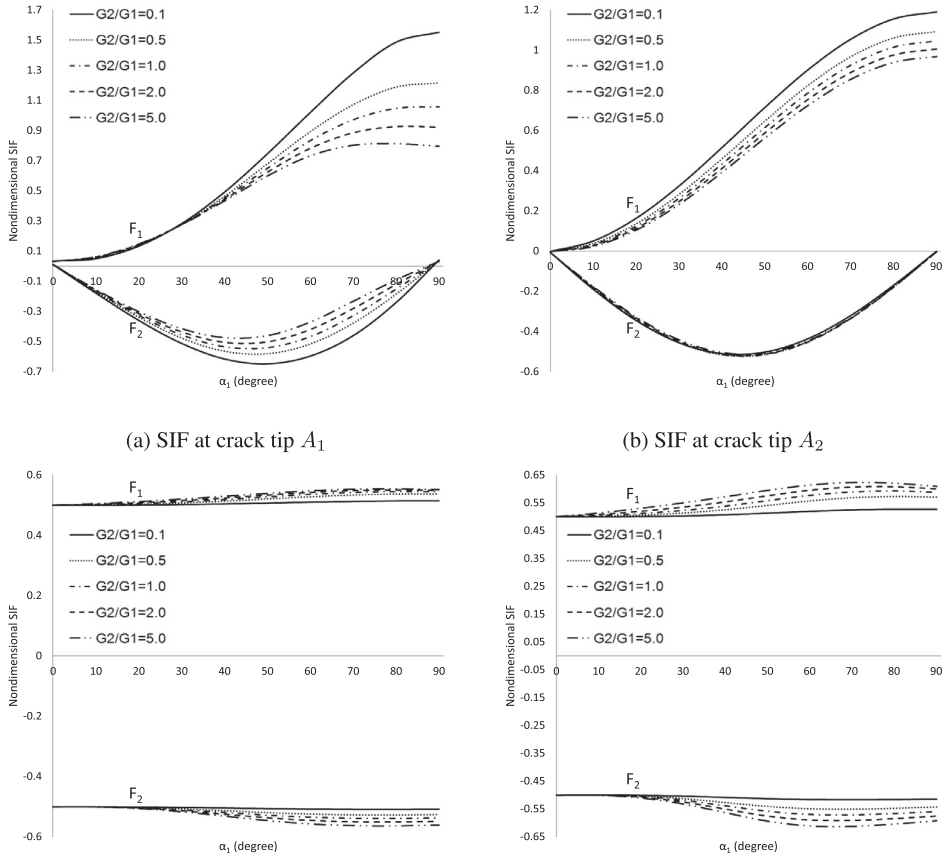

(a) SIF at crack tip A_1

(b) SIF at crack tip A_2

(c) SIF at crack tip B_1

(d) SIF at crack tip B_2

Fig. 4. Nondimensional SIF for two inclined cracks when $\alpha_2 = 45^o$ and α_1 varies (Fig. 2(b)).

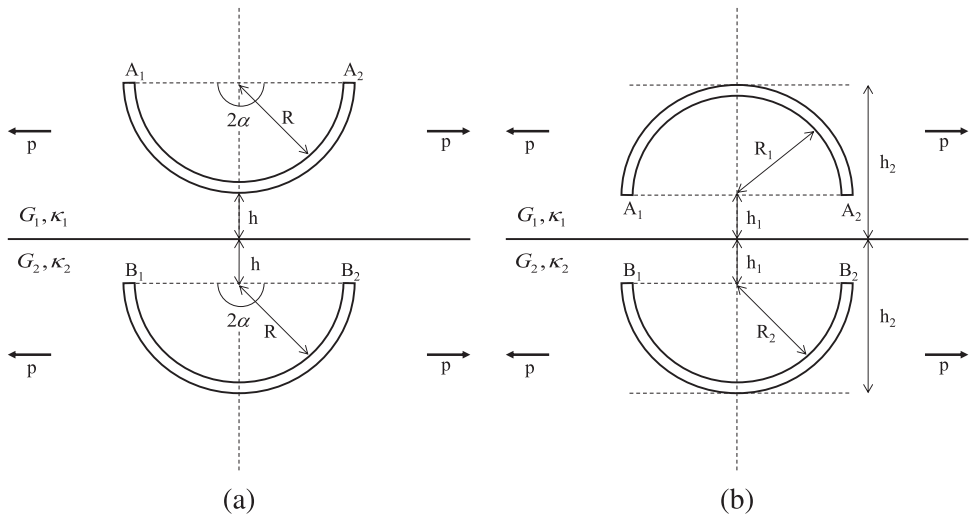

Fig. 5. Two semi circular arc cracks problems in the bonded dissimilar materials.

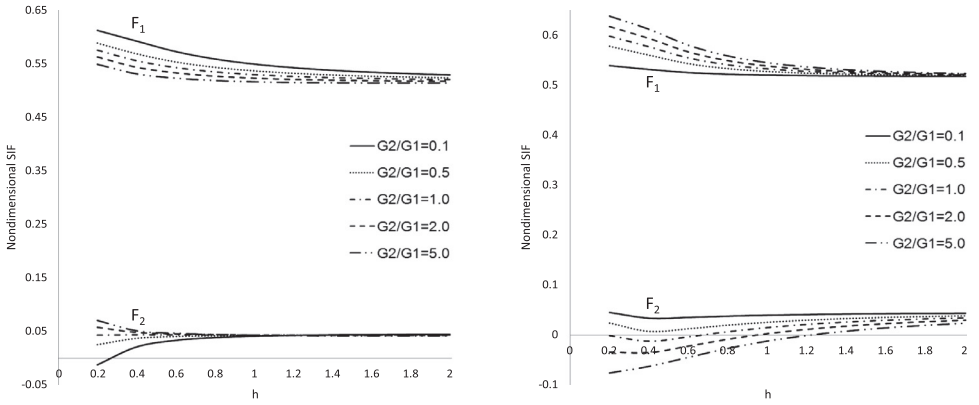

(a) SIF at the crack tip A_1 (b) SIF at the crack tip B_1

Fig. 6. Nondimensional SIF for two semi circular arc cracks with the same radius R and facing the same direction (Fig. 5(a)).

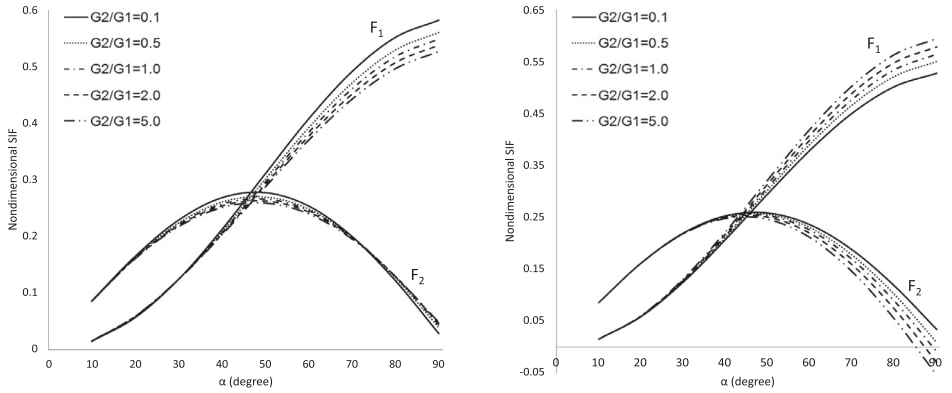

(a) SIF at the crack tip A_1 (b) SIF at the crack tip B_1

Fig. 7. Nondimensional SIF for two circular arc cracks when $h = 0.5R$ and α varies (Fig. 5(a)).

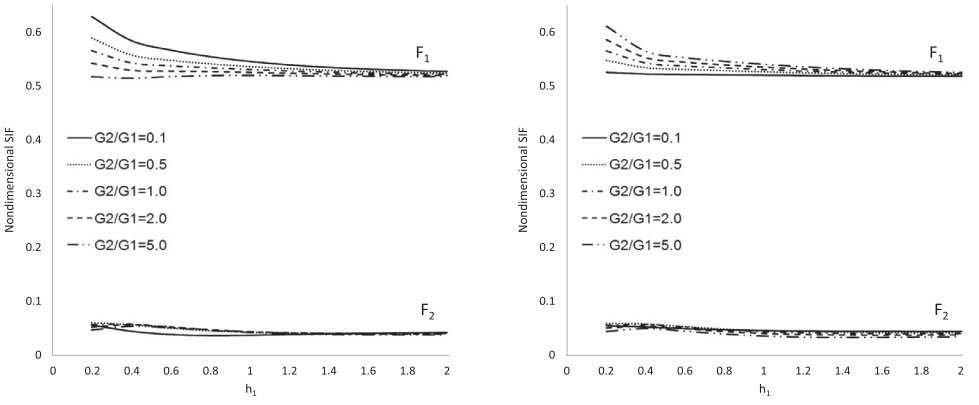

(a) SIF at the crack tip A_1 (b) SIF at the crack tip B_1

Fig. 8. Nondimensional SIF for two semi circular arc cracks facing in an opposite direction when $R_1 = R_2$ and h_1 varies (Fig. 5(b)).

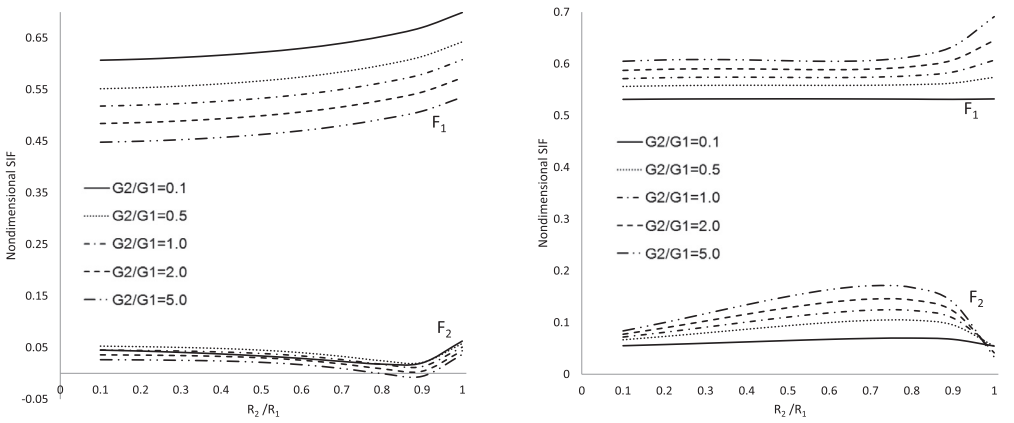

(a) SIF at the crack tip A_1 (b) SIF at the crack tip B_1

Fig. 9. Nondimensional SIF versus R_2/R_1 for two semi circular arc cracks facing in an opposite direction when $R_1/h_2 = 0.9$ and $h_2 = 1.0$ (Fig. 5(b)).

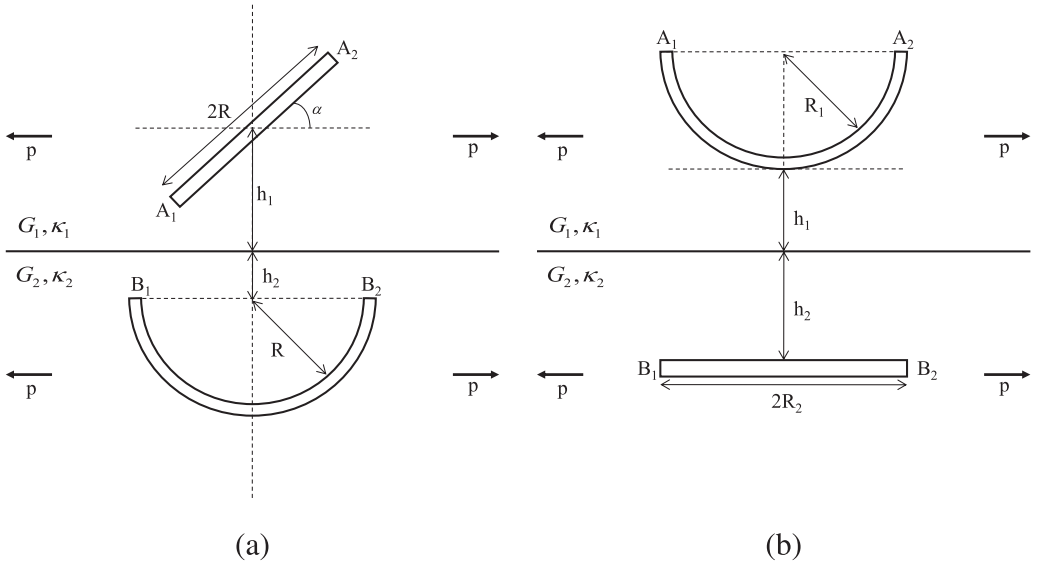

Fig. 10. An inclined crack and a semi circular arc crack in bonded dissimilar materials.

3.3. An inclined and a semi circular arc cracks

Consider an inclined crack in the upper part and a semi circular arc crack facing upward in the lower part of bonded dissimilar materials (Fig. 10(a)), and a semi circular arc crack facing upward in the upper part and a horizontal crack in the lower part (Fig. 10(b)).

Table 2 shows the nondimensional SIF for the problem in Fig. 10(a) when $R = h_2 = 1.0$, $\alpha = 90^o$ and R/h_1 varies. It is found that F_1 at crack tip B_1 is equal to F_1 at tip B_2, whereas F_2 at crack tips A_1 and A_2 is zero and F_2 at crack tip B_1 is equal to the negative of F_2 at tip B_2. Fig. 11 presents the nondimensional SIF as α varies when $R = h_2 = 1.0$ and $R/h_1 = 0.9$. It is found that at crack tip A_1, as α increases F_1 increases and F_2 decreases for $\alpha < 50^o$, and as G_2/G_1 increases F_1 decreases and F_2 increases. At crack tip A_2, as α increases F_1 increases and F_2 decreases for $\alpha < 45^o$, and as G_2/G_1 increases F_1 decreases and F_2 does not show any significant differences. At crack tip B_1, as α increases F_1 increases and F_2 decreases, and as G_2/G_1 increases F_1 increases for $\alpha > 50^o$ and F_2 decreases. Whereas at crack tip B_2, as α increases F_1 and F_2 increase, and as G_2/G_1 increases F_1 increases and F_2 increases for $\alpha > 50^o$.

Fig. 12 shows the nondimensional SIF when $h_1 = h_2 = 0.5R_2$, $R_2 = 1.0$ and R_1/R_2 varies for the problem defined in Fig. 10(b). It is observed that F_1 at crack tips A_1 and B_1 are equals to F_1 at tips A_2 and B_2, respectively, whereas F_2 at crack tips A_1 and B_1 are equals to the negative of F_2 at tips A_2 and B_2, respectively. At crack tip A_1, as R_1/R_2 increases F_1

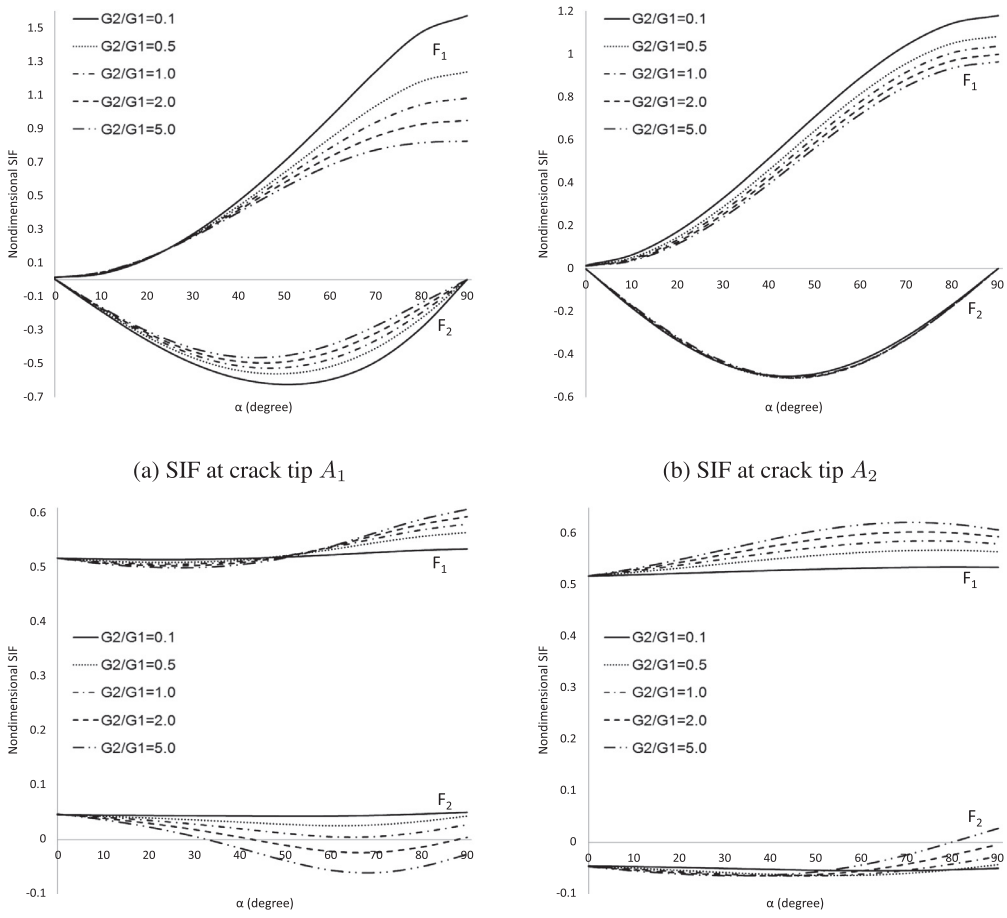

(a) SIF at crack tip A_1

(b) SIF at crack tip A_2

(c) SIF at crack tip B_1

(d) SIF at crack tip B_2

Fig. 11. Nondimensional SIF for an inclined crack and a semi circular arc crack facing upward direction, when α varies (Fig. 10(a)).

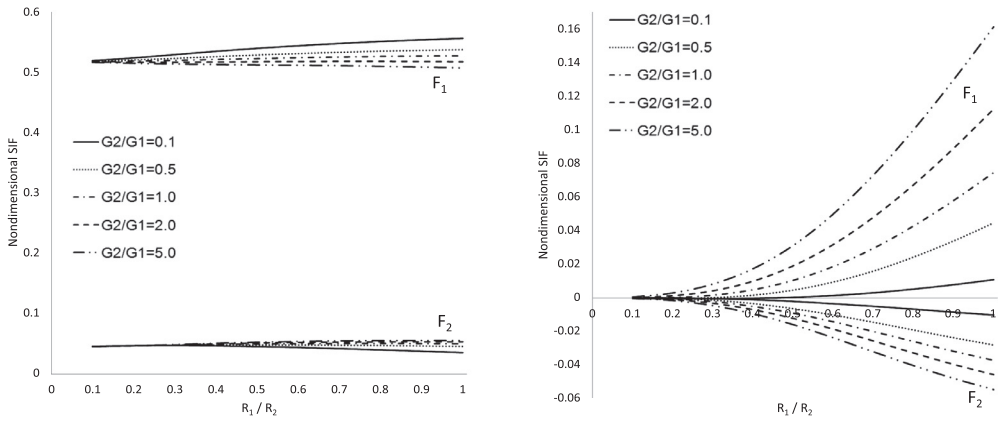

(a) SIF at the crack tip A_1

(b) SIF at the crack tip B_1

Fig. 12. Nondimensional SIF when $h_1 = h_2 = 0.5R_2$, $R_2 = 1.0$ and R_1/R_2 varies (Fig. 10(b)).

Table 2
SIF for an inclined and a semi circular arc cracks, when $R = h_2 = 1.0$ and $\alpha = 90^o$ (Fig. 10(a)).

G_2/G_1	SIF	R/h_1								
		0.1	0.2	0.3	0.4	0.5	0.6	0.7	0.8	0.9
0.1	F_{1A_1}	1.0035	1.0146	1.0341	1.0628	1.1025	1.1568	1.2334	1.3506	1.5718
	F_{1A_2}	1.0031	1.0112	1.0235	1.0391	1.0578	1.0799	1.1059	1.1373	1.1785
	F_{1B_1}	0.5174	0.5182	0.5195	0.5214	0.5236	0.5260	0.5285	0.5312	0.5342
	F_{2B_1}	0.0450	0.0442	0.0436	0.0433	0.0435	0.0443	0.0456	0.0475	0.0502
0.5	F_{1A_1}	1.0023	1.0093	1.0213	1.0380	1.0594	1.0861	1.1196	1.1647	1.2373
	F_{1A_2}	1.0019	1.0069	1.0141	1.0227	1.0324	1.0431	1.0547	1.0675	1.0820
	F_{1B_1}	0.5182	0.5209	0.5254	0.5312	0.5378	0.5447	0.5515	0.5582	0.5646
	F_{2B_1}	0.0441	0.0414	0.0384	0.0360	0.0348	0.0350	0.0365	0.0393	0.0431
1.0	F_{1A_1}	1.0015	1.0063	1.0140	1.0242	1.0358	1.0479	1.0597	1.0707	1.0806
	F_{1A_2}	1.0013	1.0044	1.0087	1.0135	1.0184	1.0233	1.0281	1.0324	1.0365
	F_{1B_1}	0.5189	0.5233	0.5298	0.5379	0.5467	0.5558	0.5646	0.5727	0.5800
	F_{2B_1}	0.0435	0.0392	0.0340	0.0292	0.0256	0.0237	0.0234	0.0247	0.0272
2.0	F_{1A_1}	1.0009	1.0034	1.0073	1.0114	1.0140	1.0132	1.0060	0.9881	0.9480
	F_{1A_2}	1.0006	1.0020	1.0037	1.0050	1.0057	1.0055	1.0044	1.0020	0.9982
	F_{1B_1}	0.5199	0.5262	0.5349	0.5451	0.5560	0.5669	0.5772	0.5863	0.5937
	F_{2B_1}	0.0429	0.0367	0.0286	0.0204	0.0132	0.0079	0.0046	0.0033	0.0039
5.0	F_{1A_1}	1.0001	1.0004	1.0004	0.9985	0.9923	0.9788	0.9534	0.9085	0.8245
	F_{1A_2}	1.0000	0.9996	0.9986	0.9964	0.9929	0.9880	0.9814	0.9732	0.9630
	F_{1B_1}	0.5213	0.5300	0.5411	0.5535	0.5663	0.5789	0.5903	0.6000	0.6071
	F_{2B_1}	0.0422	0.0336	0.0217	0.0088	−0.0034	−0.0136	−0.0211	−0.0257	−0.0274

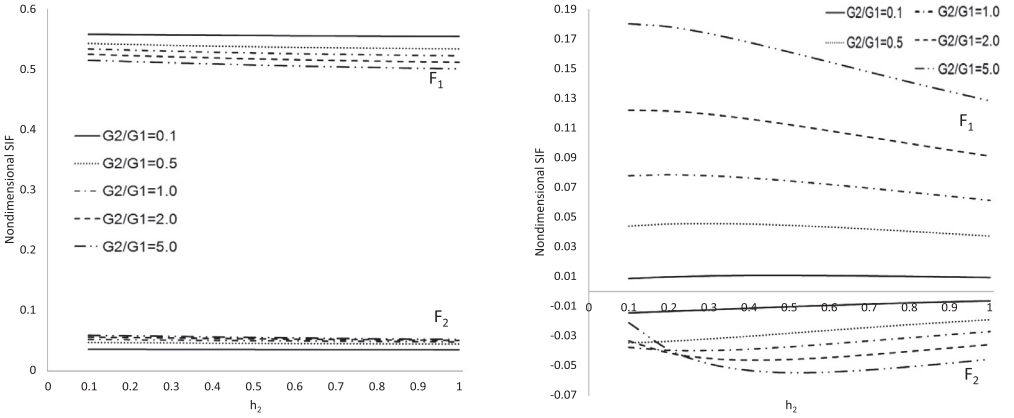

(a) SIF at the crack tip A_1 (b) SIF at the crack tip B_1

Fig. 13. Nondimensional SIF when $h_1 = 0.5R_1$, $R_1 = R_2 = 1.0$ and h_2 varies (Fig. 10(b)).

increases and F_2 does not show any significant differences, and as G_2/G_1 increases F_1 decreases and F_2 increases. Whereas at crack tip B_1, as R_1/R_2 increases F_1 increases and F_2 decreases, and as G_2/G_1 increases F_1 increases and F_2 decreases. For $h_1 = 0.5R_1$, $R_1 = R_2 = 1.0$ and h_2 varies the nondimensional SIF are presented in Fig. 13. It is found that at crack tip A_1, as h_2 increases F_1 and F_2 does not show any significant differences, and as G_2/G_1 increases F_1 decreases and F_2 increases. Whereas at crack tip B_1, as h_2 increases F_1 decreases and F_2 increases, and as G_2/G_1 increases F_1 increases and F_2 decreases.

3.4. A circular arc and a perpendicular cracks

Consider a circular arc crack in the upper part and a perpendicular crack in the lower part of bonded dissimilar materials subjected to remote shear stress $\sigma_{x_1} = \sigma_{x_2} = p$ defined in Fig. 14.

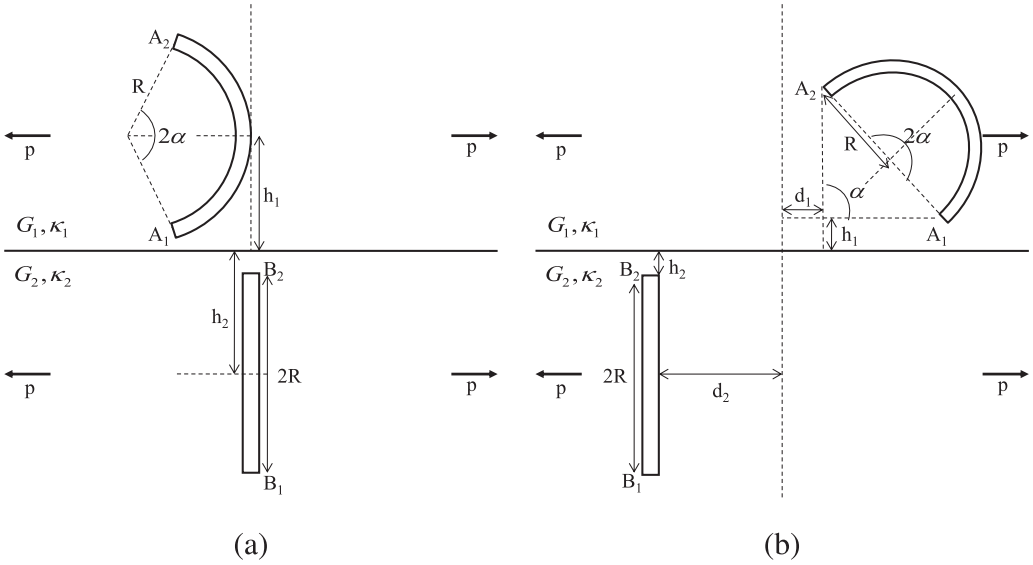

Fig. 14. A circular arc and a perpendicular cracks in bonded dissimilar materials.

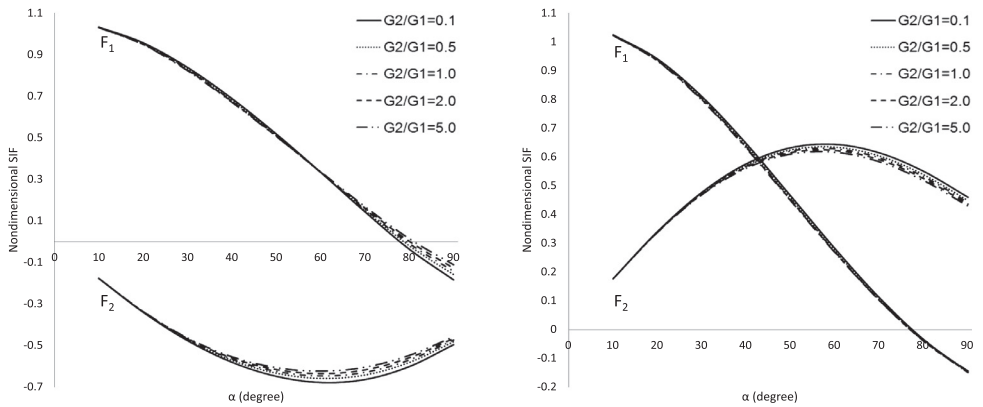

(a) SIF at crack tip A_1

(b) SIF at crack tip A_2

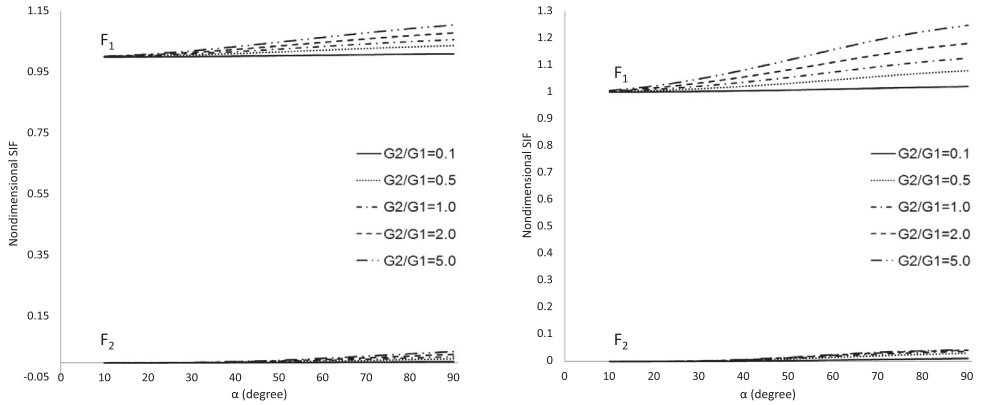

(c) SIF at crack tip B_1

(d) SIF at crack tip B_2

Fig. 15. Nondimensional SIF when $h_1 = 2R$, $R/h_2 = 0.9$ and α varies (Fig. 14(a)).

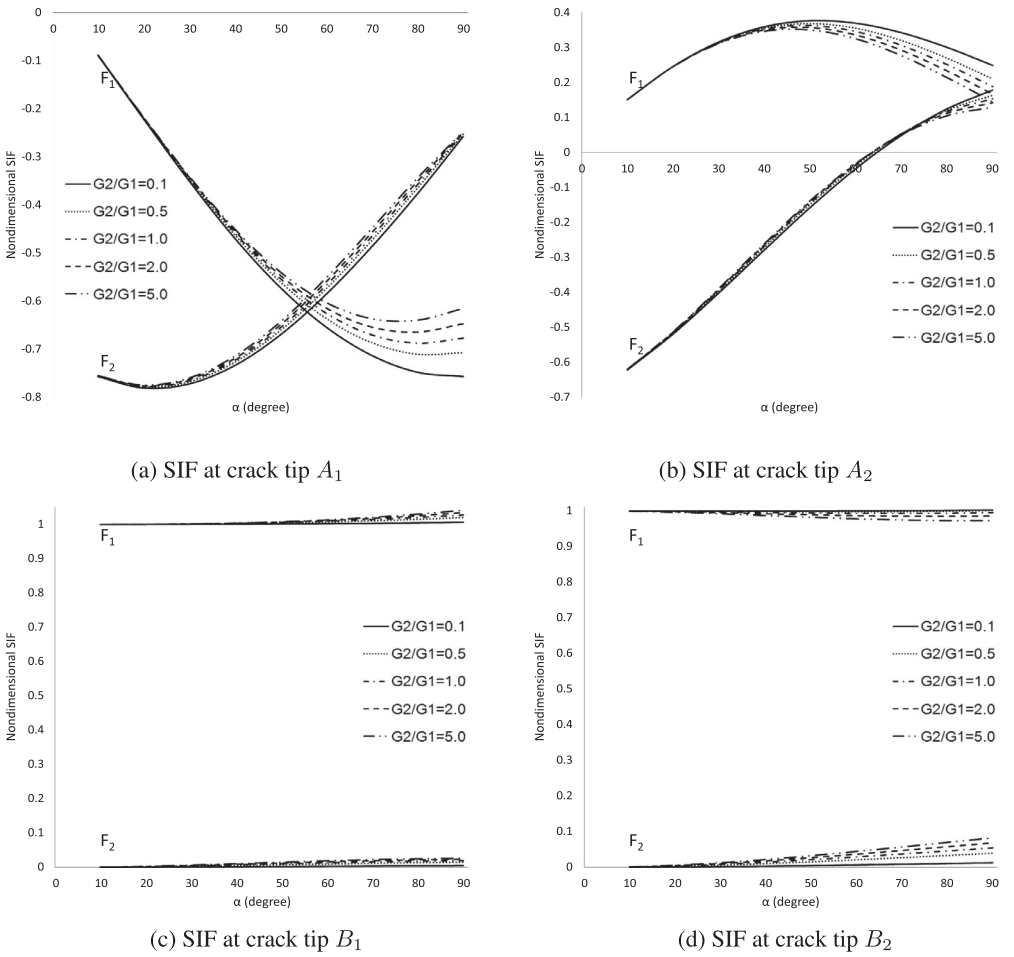

(a) SIF at crack tip A_1

(b) SIF at crack tip A_2

(c) SIF at crack tip B_1

(d) SIF at crack tip B_2

Fig. 16. SIF when $d_1 = h_1 = 0.5R,\ 9d_2 = 10R,\ 9h_2 = 1$ and α varies (Fig. 14(b)).

Fig. 15 presents the nondimensional SIF when $h_1 = 2R,\ R/h_2 = 0.9$ and α varies for the problem defined in Fig. 14(a). It is found that at crack tip A_1, as α increases F_1 decreases and F_2 decreases for $\alpha < 60^o$, and as G_2/G_1 increases F_1 does not show any significant differences and F_2 increases. At crack tip A_2, as α increases F_1 decreases and F_2 increases for $\alpha < 60^o$, and as G_2/G_1 increases F_1 does not show any significant differences and F_2 decreases. At crack tip B_1, as α increases F_1 increases and F_2 does not show any significant differences, and as G_2/G_1 increases F_1 increases and F_2 does not show any significant differences. Whereas F_1 and F_2 at crack tip B_2 behave as F_1 and F_2 at crack tip B_1.

Fig. 16 shows the nondimensional SIF for the problem defined in Fig. 14(b) when $d_1 = h_1 = 0.5R,\ 9d_2 = 10R,\ 9h_2 = 1$ and α varies. At crack tip A_1, as α increases F_1 decreases and F_2 increases, and as G_2/G_1 increases F_1 and F_2 increase. At crack tip A_2, as α increases F_1 increases for $\alpha < 50^o$ and F_2 increases, and as G_2/G_1 increases F_1 decreases and F_2 does not show any significant differences. At crack tip B_1, as α and G_2/G_1 increase F_1 and F_2 does not show any significant differences. Whereas at crack tip B_2, as α increases F_1 does not show any significant differences and F_2 increases, and as G_2/G_1 increase F_1 decreases and F_2 increases. Fig. 17 presents the nondimensional SIF when $d_1 = d_2 = R,\ \alpha = 90^o$ and $h_1 = h_2$ varies (Fig. 14(b)). It is observed that at crack tip A_1, as $h_1 = h_2$ increases F_1 increases for $G_2/G_1 < 1.0$ and decreases for $G_2/G_1 \geq 1.0$ and F_2 increases, and as G_2/G_1 increases F_1 increases and F_2 does not show any significant differences. At crack tip A_2, as $h_1 = h_2$ increases F_1 increases for $G_2/G_1 > 0.0$ and decreases for $G_2/G_1 = 0.0$ and F_2 decreases, and as G_2/G_1 increases F_1 and F_2 decrease. At crack tip B_1, as $h_1 = h_2$ increases F_1 and F_2 does not show any significant differences, and as G_2/G_1 increases F_1 increases and F_2 does not show any significant differences. Whereas at crack tip B_2, as $h_1 = h_2$ increases F_1 does not show any significant differences and F_2 decreases, and as G_2/G_1 increases F_1 decreases for $h_1 = h_2 < 0.6$ and increases for $h_1 = h_2 > 0.6$ and F_2 increases.

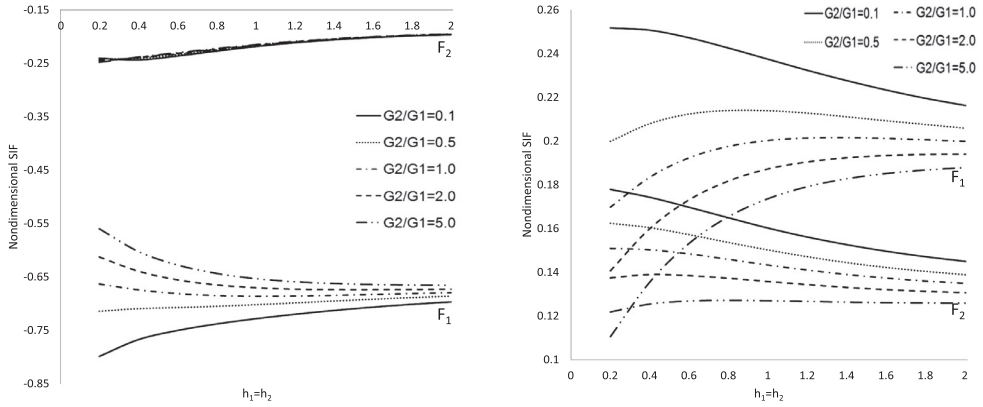

(a) SIF at crack tip A_1 (b) SIF at crack tip A_2

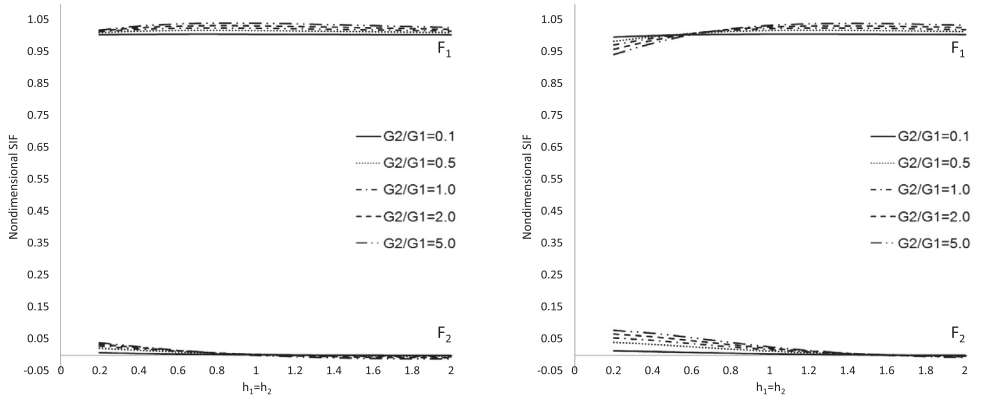

(c) SIF at crack tip B_1 (d) SIF at crack tip B_2

Fig. 17. Nondimensional SIF when $d_1 = d_2 = R$, $\alpha = 90^o$ and $h_1 = h_2$ varies (Fig. 14(b)).

4. Conclusions

In this paper, the new system of HSIEs for the multiple cracks problems in both upper and lower parts of bonded dissimilar materials are formulated by using the modified complex variable function method with the crack opening displacement function as the unknown. Our new system of HSIEs reduces to the system of HSIEs for cracks problems in an infinite plane when $G_1 = G_2$. Numerical calculation shows that the Mode I and Mode II nondimensional SIF for cracks in both upper and lower parts of bonded dissimilar materials depend on the elastic constants ratio (G_2/G_1), cracks geometries and the distance between the crack and the boundary. However the position and geometries of the cracks are more influence on the variations of nondimensional SIF.

Acknowledgments

The first author would like to thanks the Ministry of Education Malaysia, Universiti Putra Malaysia and Universiti Teknikal Malaysia Melaka for the financial support. The second author would like to thank the Universiti Putra Malaysia for Putra Grant, project no: 9567900 and Fundamental Research Grant Scheme (FRGS) project no: 01-01-16-18685R5524975.

References

[1] M.R. Aridi, N.M.A.N. Long, Z.K. Eshkuvatov, Stress intensity factor for the interaction between a straight crack and a curved crack in plane elasticity, Acta Mechanica Solida Sinica 29 (4) (2016) 1–9.
[2] N.M.A.N. Long, Z.K. Eshkuvatov, Hypersingular integral equation for multiple curved cracks problem in plane elasticity, Int. J. Solids Struct. 46 (2009) 2611–2617.
[3] T. Zheng, Z. Zhu, B. Wang, L. Zeng, Stress intensity factor for an infinite plane containing three collinear cracks under compression, ZAMM J. Appl. Math. Mech. 94 (10) (2014) 853–861.

[4] R.A. Rafar, N.M.A.N. Long, N. Senu, N.A. Noda, Stress intensity factor for multiple inclined or curved cracks problem in circular positions in plane elasticity, ZAMM J. Appl. Math. Mech. 97 (11) (2017) 1482–1494.
[5] N.R.F. Elfakhakhre, N.M.A.N. Long, Z.K. Eshkuvatov, Numerical solutions for cracks in an elastic half plane, Acta Mech. Sin. 35 (1) (2019) 212–227.
[6] Y.Z. Chen, Y.K. Cheung, New integral equation approach for the crack problem in elastic half-plane, Int. J. Fract. 46 (1990) 57–69.
[7] Y.Z. Chen, Evaluation of the t-stress for multiple cracks in an elastic half-plane using singular integral equation and Green's function method, Appl. Math. Comput. 228 (2014) 17–30.
[8] N.R.F. Elfakhakhre, N.M.A.N. Long, Z.K. Eshkuvatov, Stress intensity factor for an elastic half plane weakened by multiple curved cracks, Appl. Math. Modell. 60 (2018) 540–551.
[9] H. Ferdjani, R. Abdelmoula, Propagation of a dugdale crack at the edge of a half plane, Control Mech. Thermodyn. 30 (1) (2018) 195–205.
[10] Y.Z. Chen, Multiple crack problems for two bonded half planes in plane and antiplane elasticity, Eng. Fracture Mech. 25 (1) (1986) 1–9.
[11] Y.Z. Chen, N. Hasebe, Stress-intensity factors for curved circular crack in bonded dissimilar materials, Theor. Appl. Fract. Mech. 17 (1992) 189–196.
[12] M. Isida, H. Noguchi, Arbitrary array of cracks in bonded half planes subjected to various loadings, Eng. Fract. Mech. 46 (3) (1993) 365–380.
[13] Y.Z. Chen, X.Y. Lin, X.Z. Wang, Numerical solution for curved crack problem in elastic half-plane using hypersingular integral equation, Philosoph. Mag. 89 (26) (2009) 2239–2253.
[14] Y.K. Cheung, Y.Z. Chen, New integral equation for plane elasticity crack problems, Theor. Appl. Fract. Mech. 7 (1987) 177–184.
[15] N.R.F. Elfakhakhre, N.M.A.N. Long, Z.K. Eshkuvatov, Stress intensity factor for multiple cracks in half plane elasticity, in: Proceedings of the AIP Conference, 1795, 2017, pp. 1–8.
[16] Y.Z. Chen, New fredholm integral equation for multiple crack problem in plane elasticity and antiplane elasticity, Int. J. Fract. 64 (1993) 63–77.
[17] I.N. Sneddon, S.C. Das, The stress intensity factor at the tip of an edge crack in an elastic half-plane, Int. J. Eng. Sci. 9 (1) (1971) 25–36.
[18] M. Isida, H. Noguchi, Distributed cracks and kinked cracks in bonded dissimilar half planes with an interface crack, Int. J. Fract. 66 (4) (1994) 313–337.
[19] K.B. Hamzah, N.M.A.N. Long, N. Senu, Z.K. Eshkuvatov, M.R. Ilias, Stress intensity factors for a crack in bonded dissimilar materials subjected to various stresses, Univ. J. Mech. Eng. 7 (4) (2019) 179–189.
[20] H. Yu, L. Wu, L. Guo, S. Du, Q. He, Investigation of mixed-mode stress intensity factors for nonhomogeneous materials using an interaction integral method, Int. J. Solids Struct. 46 (2009) 3710–3724.
[21] K.B. Hamzah, N.M.A.N. Long, N. Senu, Z.K. Eshkuvatov, Stress intensity factor for multiple cracks in bonded dissimilar materials using hypersingular integral equations, Appl. Math. Modell. 73 (2019) 95–108.
[22] Y. Li, E. Viola, Size effect investigation of a central interface crack between two bonded dissimilar materials, Comp. Struct. 105 (2013) 90–107.
[23] R. Ghajar, S. Peyman, J. Sheikhi, M. Poorjamshidian, Numerical investigation of the mixed-mode stress intensity factors in FGMs considering the effect of graded poisson's ratio, J. Solid Mech. 9 (1) (2017) 172–185.
[24] B. Serier, M. Belhouari, B.B. Bouiadjra, Numerical study of the interaction between an interfacial crack and a subinterfacial microcrack in bi-materials, Comput. Mater. Sci. 29 (2004) 309–314.
[25] Y. Wang, H. Waisman, Material dependent crack-tip enrichment functions in XFEM for modeling interfacial cracks in bimaterials, Int. J. Numer. Methods Eng. 112 (11) (2017) 1495–1518.
[26] S. Itou, Stress intensity factors for four interface-close cracks between a nonhomogeneous bonding layer and one of two dissimilar elastic half-planes, Eur. J. Mech. A/Solids 59 (2016) 242–251.
[27] M. Paggi, J. Reinoso, Revisiting the problem of a crack impinging on an interface: a modeling framework for the interaction between the phase field approach for brittle fracture and the interface cohesive zone model, Comput. Methods Appl. Mech. Eng. 321 (2017) 145–172.
[28] X. Lan, S. Ji, N.A. Noda, Y. Cheng, Stress intensity factor solutions for several crack problems using the proportional crack opening displacements, Eng. Fracture Mech. 171 (2017) 35–49.
[29] S.G.F. Cordeiro, E.D. Leonel, Mechanical modelling of three-dimensional cracked structural components using the isogeometric dual boundary element method, Appl. Math. Modell. 63 (2018) 415–444.
[30] H.D.C.e. Andrade, E.D. Leonel, The multiple fatigue crack propagation modelling in nonhomogeneous structures using the DBEM, Eng. Anal. Boundary Elements 98 (2019) 296–309.
[31] Y.Z. Chen, N. Hasebe, Properties of eigenfunction expansion form for the rigid line problem in dissimilar media, Int. J. Solids Struct. 33 (5) (1996) 611–628.
[32] X. Han, F. Ellyin, Z. Xia, A crack near the interface of bonded elastic-viscoelastic planes, Int. J. Solids Struct. 38 (2001) 3453–3468.
[33] X. Han, F. Ellyin, Z. Xia, Interaction among interface, multiple cracks and dislocations, Int. J. Solids Struct. 39 (2002) 1575–1590.
[34] N.I. Muskhelishvili, Some Basic Problems of the Mathematical Theory of Elasticity, Noordhoff International Publishing, Leyden, 1953.